



24th COBEM - 2017



24th ABCM International Congress of Mechanical Engineering
December 3-8, 2017, Curitiba, PR, Brazil

COBEM-2017-0277

MEASURING AND COMPARING THE IGNITION DELAY TIMES OF DIESEL, ETHANOL ADDITIVE AND BIODIESEL USING A SHOCK TUBE.

Claudio Marcio Santana

Jose Eduardo Mautone Barros

Helder Alves de Almeida Junior

Universidade Federal de Minas Gerais - Av. Antonio Carlos, 6627, Pampulha, Belo Horizonte – CEP: 31270-901

Claudiowsantana@gmail.com

mautone@demec.ufmg.br

helder.alves.eng@gmail.com

Abstract. *The objective of this work is correlate the ignition delay times of Diesel S25 (25ppm), ethanol with 5% additive increase cetane number, Biodiesel B100 and Diesel reference measured in a shock tube. The results were correlated with the cetane number of respective fuels and compared with the ignition delay times of Diesel and Biodiesel with cetane numbers of known. The shock tube is a metal tube that the gas at low pressure and high pressure are separated by a diaphragm. When the diaphragm (make of material copper and aluminum) breaks on predetermined conditions (high pressure in this case) produces shock waves that move from the high-pressure chamber (known the compression chamber or Driver section) for low pressure chamber (known the expansion chamber or Driven section). The tests were performed under the following initial conditions of the Driver section: 30 bar of pressure breakup diaphragm and temperature of 100 °C. For determining and recording the ignition delay time was used pressure sensors with high acquisition rate (differential sensors) and detect flame sensor. With information from pressure sensors and flame sensor the ignition delay time was determined. Is measured ignition delay times of ethanol additive, Diesel S25, Diesel reference and biodiesel B100. Was concluded that the ignition delay time of ethanol with 5% additive was twice large that ignition delay time Diesel S25. The ignition delay time of biodiesel B100 was approximately four times greater than the ignition delay time of Diesel S25. The ignition delay time of the Diesel reference was smaller than the S25.*

Keywords: *Shock Tube, Combustion, Ignition Delay Time, Driver section, Driven section.*

1. INTRODUCTION

A shock tube is a device used to create the gas flow in order to simulate conditions of dynamic fluid flow. The simple configuration of shock tube is a tube of great length with constant cross-sectional area formed by two closed sections and separated by a diaphragm (Antonio, M. C. N.,2001). The figure 1 shows the design of a simple shock tube.

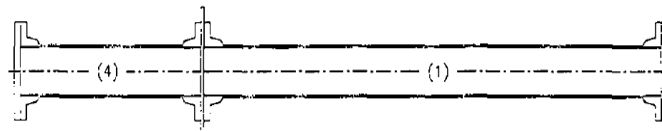


Figure 1 - Simple shock tube.

The First section is called Driver section is filled with a gas or gas mixture until determined pressure, while another section called Driven remains at low pressure than the Driver section. When the pressure difference between the two sections is sufficient to makes the diaphragm rupture and a shock compression wave is driven toward the low-pressure section (Driven). Instantly a wave of expansion propagates toward the high-pressure section (Driver). The gases in the sections may or may not be from the same species as may or may not be at different temperatures before rupture of the diaphragm. After the rupture of the diaphragm compression shock wave causes movement of the mass of gas increasing the temperature and pressure in the section Driven. The wave of expansion decreases the temperature and pressure of

the gas when it moves to the Driver section (Mcmillan, R.J.,2004). The figure 2 shows the sections of high and low-pressure shock tube before the rupture of the diaphragm.

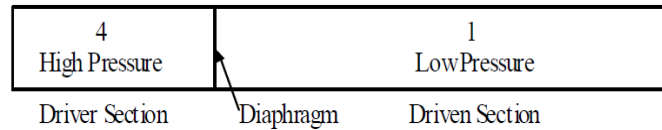


Figure 2 - Representation of the sections of the shock tube before rupture of the diaphragm.

Immediately after rupture of the diaphragm form a region called the contact surface on which the gas sections are Driven and Driver and begin to mix. With the movement of the gas mass inside the tube that region disappears (Mcmillan, R.J.,2004). The figure 3 shows the regions formed between the contact surfaces after rupture of the diaphragm.

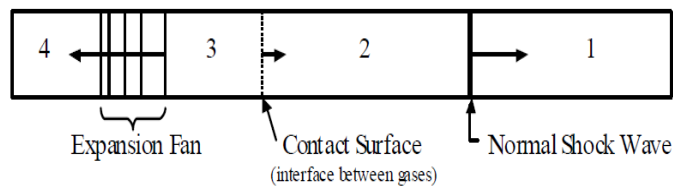


Figure 3 - Formation of the contact surface immediately after rupture of the diaphragm.

The compression wave (also called an incident) propagates to the right end of the tube, this movement causes increase temperature and pressure of the gas in the section Driven. When the compression wave achieves the closed end of the tube the shock wave reflected and propagates toward the other end of the tube. In the movement of back the reflected wave find with the incident wave, the superposition of shock waves increases more the temperature and pressure of the gas in the Driven section. The reflected wave is responsible for causing often the dissociation and ionization of air. Also, the expansion wave moves toward the other end of the tube. When it reaches the end, also closed, the wave is reflected and propagates back to the center of the tube. This process continues until the gas pressure and temperature to stabilize, which typically lasts less than one second (Mcmillan, R.J.,2004).

The figure 4 shows the propagation of the shock wave, shock wave reflected, expansion wave, reflected expansion wave and the contact surface as a function of time after the rupture of the diaphragm shock tube.

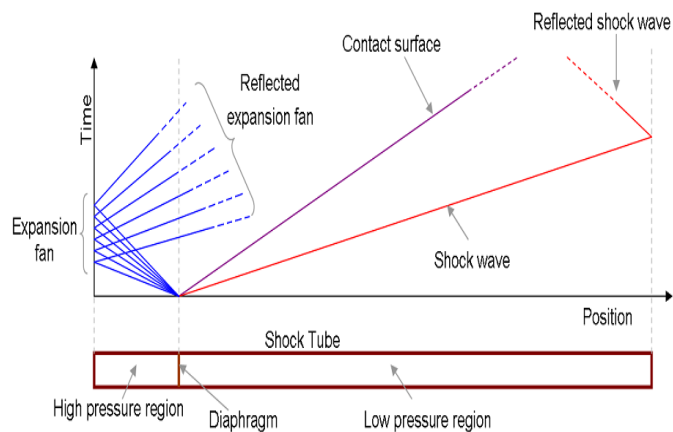


Figure 4 - Propagation of shock wave and expansion after rupture of the diaphragm Tube Shock.

There are two parameters that determine the strength of the shock the pressure ratio between the sections Diver and Driven (P_4/P_1) and speed ratio of propagation of sound in the respective sections Driver and Driven (a_4/a_1). The ratio of the speed of sound is determined by the ratio of specific heats and molecular weights of the gases used in sections Driver and Driven (Mcmillan, R.J.,2004). The figure 5 represents the conditions of shock tube before rupture of the diaphragm, assuming that the two sections are at the same temperature.

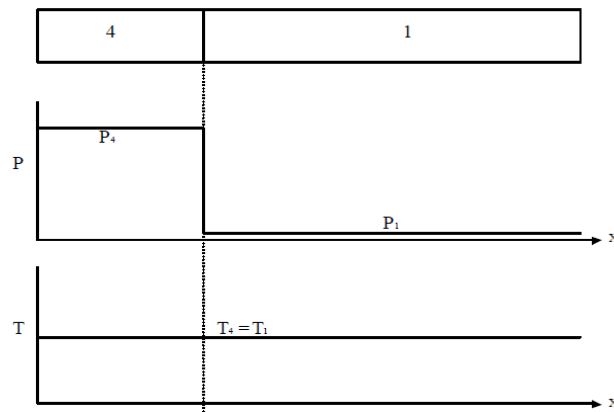


Figure 5 - Condition shock tube before rupture of the diaphragm.

The principles of normal movement of the shock are used to develop the relationships between the regions 1 and 2 on each side of the compression wave and between regions 3 and 4 each side of the expansion wave. Although initially there are only two gases in the tube, after the rupture of the diaphragm there are four states gas temperature, pressure, density and specific heat well defined for each region. The front of the shock wave and expansion wave the pressure, density and temperature are the same initial conditions sections of low and high pressure respectively, these regions are not affected by shock wave and expansion wave. Behind the shock wave the pressure, density and temperature increase, while behind the expansion surface these variables decrease. The region bounded by the shock wave and expansion wave is known as the contact surface. The figure 6 shows the conditions of shock tube after rupture of the diaphragm.

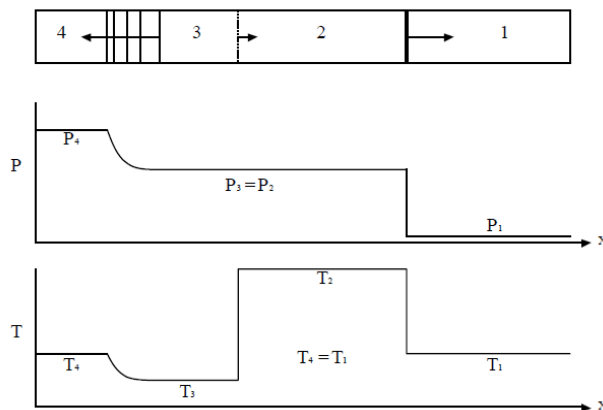


Figure 6 - Conditions Tube Shock after diaphragm rupture.

The reflected shock wave travels at a higher speed and pressure than the incident wave (Mcmillan, R.J.,2004). The figure 7 shows the conditions of shock tube after reflection of the shock wave.

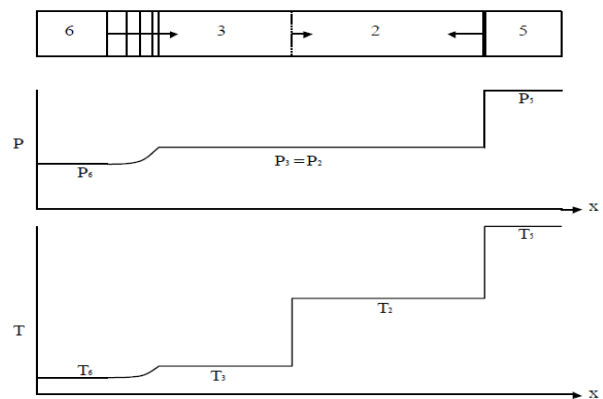


Figure 7- Conditions of shock tube after reflection of the shock wave.

The speed of sound for each state gas must be calculated using the Eq. (1).

$$a = \sqrt{\gamma RT} \quad (1)$$

γ is the ratio of specific heats of the gas, R is the universal gas constant and T is the gas temperature in the respective regions of the tube. The Mach number can be determined using the following Eq. (2) (Mcmillan, R.J.,2004).

$$\frac{P_4}{P_1} = \frac{\gamma_{1-1}}{\gamma_{1+1}} \left[\frac{2\gamma_1}{\gamma_{1-1}} M_s^2 - 1 \right] \left[1 - \frac{\frac{\gamma_{4-1}}{\gamma_{4+1}} \left(\frac{a_1}{a_4} \right) (M_s^2 - 1)}{M_s} \right]^{\frac{2\gamma_4}{\gamma_{4-1}}} \quad (2)$$

Where M_s is the Mach number of the shock wave, the subscript 1 denotes the properties of the Driven section and the subscript 4 denotes the properties of the Driver section. With the Mach number known to the pressure ratio on both sides of the shock wave (P_2/P_1) can be calculated using the ratio shock wave given for Eq. (3) (Mcmillan, R.J.,2004).

$$\frac{P_2}{P_1} = 1 + \frac{2\gamma_1}{\gamma_1 + 1} (M_s^2 - 1) \quad (3)$$

The pressure ratio (P_2/P_1) can be used to determine the temperature ratio (T_2/T_1) on both sides of the shock wave given for Eq. (4) (Mcmillan, R.J.,2004).

$$\frac{T_2}{T_1} = \frac{P_2}{P_1} \left(\frac{\frac{\gamma_1 + 1}{\gamma_1 - 1} + \frac{P_2}{P_1}}{1 + \frac{\gamma_1 + 1}{\gamma_1 - 1} \frac{P_2}{P_1}} \right) \quad (4)$$

The temperature of the gas behind the shock wave can be used to predict the dissociation and ionization of the air. The relationship between gas pressure and shock Mach number is asymptotic. Therefore, for each pair of gases Mach number there is a theoretical can be achieved. This theoretical maximum number indicated by a star subscribed can be calculated by Eq. (5) (Mcmillan, R.J.,2004).

$$M_s^* = \frac{\gamma_1 + 1}{2(\gamma_4 - 1)} \frac{a_1}{a_4} + \sqrt{\left[\frac{\gamma_1 + 1}{2(\gamma_4 - 1)} \frac{a_1}{a_4} \right]^2 + 1} \quad (5)$$

The velocity of the shock wave reflected depend the velocity of the incident shock wave and can be determined by the following Eq. 6 (Mcmillan, R.J.,2004).

$$\frac{M_R}{M_R^2 - 1} = \frac{M_s}{M_s^2 - 1} \sqrt{1 + \frac{2(\gamma_1 - 1)}{(\gamma_1 + 1)^2} (M_s^2 - 1) \left(\gamma_1 + \frac{1}{M_s^2} \right)} \quad (6)$$

The increased pressure of the shock wave reflected depend the speed of the incident shock wave, this ratio can be calculated by the Eq. 7 (Mcmillan, R.J.,2004).

$$\frac{P_5}{P_2} = 1 + \frac{2\gamma_1}{\gamma_1 + 1} (M_R^2 - 1) \quad (7)$$

The shock wave reflected stops the motion of the mass of gas, so that the propagation velocities of the gases behind the shock wave and the reflected shock wave front incident tend to zero. The equation (8) shows the relationship of movement of these gases (Mcmillan, R.J.,2004).

$$\frac{2a_1}{\gamma_1 + 1} \left(M_s - \frac{1}{M_s} \right) = \frac{2a_2}{\gamma_1 + 1} \left(M_R - \frac{1}{M_R} \right) \quad (8)$$

The calculations involving speed of the gas molecules are simple and can be determined by the Eq. (9) (McMillan, R.J.,2004).

$$Mach\ M = \frac{V}{a} \quad (9)$$

To calculation of the actual speed of the shock wave, this can be calculated by the Eq. (10) (McMillan, R.J.,2004).

$$V_R = M_R a_2 - V_2 \quad (10)$$

To determine the relationship between pressure of reflected shock wave and incident shock wave using only the incident the following Eq. (11) can be used (McMillan, R.J.,2004).

$$\frac{P_5}{P_2} = \left(\frac{\frac{\gamma_1 + 1}{\gamma_1 - 1} + 2 - \frac{P_1}{P_2}}{1 + \frac{\gamma_1 + 1}{\gamma_1 - 1} \frac{P_1}{P_2}} \right) \quad (11)$$

With the ratio compression known the ratio temperature of reflected shock wave and incident shock wave can be determined by Eq. (12) (McMillan, R.J.,2004).

$$\frac{T_5}{T_2} = \frac{P_5}{P_2} \left(\frac{\frac{\gamma_1 + 1}{\gamma_1 - 1} + \frac{P_5}{P_2}}{1 + \frac{\gamma_1 + 1}{\gamma_1 - 1} \frac{P_5}{P_2}} \right) \quad (12)$$

The temperature and pressure behind the reflected shock wave can be calculated knowing only the Mach number of the incident shock wave. This value can be determined from the velocity of the gas driven and wave velocity (McMillan, R.J.,2004).

2 - EXPERIMENTAL PROCEDURE

The experimental procedure involved the instrumentation of the shock tube with three pressure sensors, flame detection sensor and fuel injector. The Figure 8 shows the position of the sensors in shock tube.

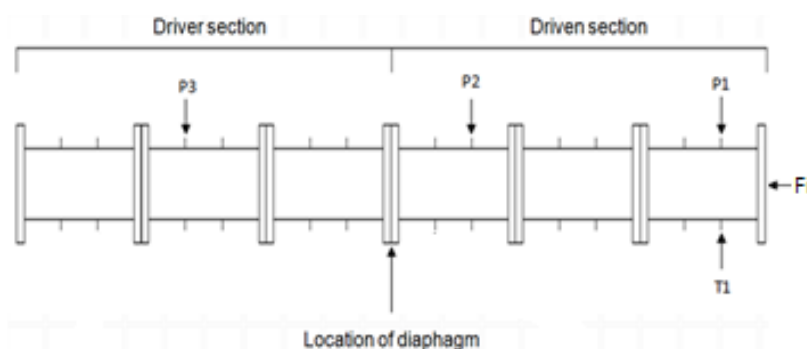


Figure 8 - Position of the sensors in shock tube.

The pressure sensor P3 monitors the pressure in the Driver section and the diaphragm rupture pressure, the pressure sensor P2 indicates the moment of passage of shock wave after diaphragm rupture, this information is used to control and define the fuel injection timing, the pressure sensor P1 shows the moment of passage of shock in region 1 where combustion occurs, the flame detection sensor T1 indicates the moment of combustion occur and the fuel injector FI which inject fuel in shock tube when the sensor pressure P2 feel the passage of shock wave. The sensors P1 and T1 are in the same position. The ignition delay time was calculated by the time difference between the passage of the shock wave by the sensor P1 and the start of the ignition detected by the flame sensor detection T1. Figure 9 shows the curve of the sensors P1 and T1 as well the time interval (Δt) which represents ignition delay time.

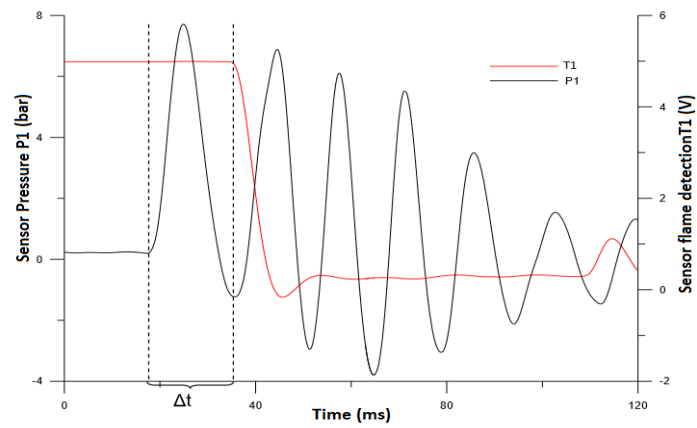


Figure 9 - Sensors P1, T1 and (Δt) which represents ignition delay time.

The figure 10 shows the general view of the shock tube where the experimental test was conducted. The figure 11 shows the last part of shock where combustion process occurs.



Figure 10 - General view of the shock tube.

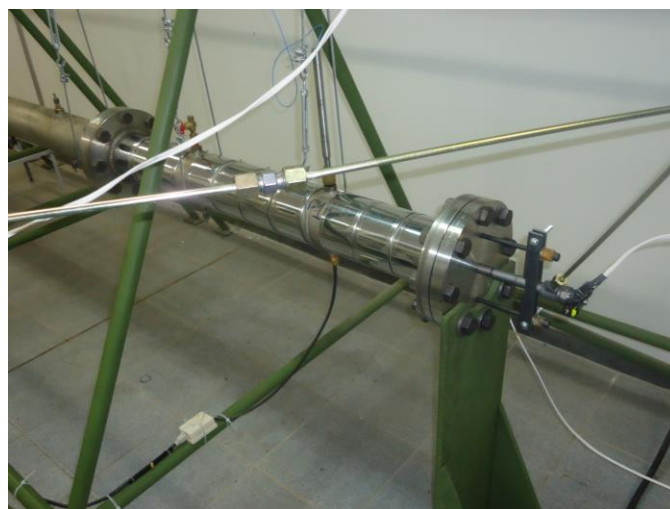


Figure 11 – Pressure sensor, flame detection flame and fuel injector of the shock tube.

The tests with combustion were performed with an acquisition rate of 40000 Hz. The tests were realized with 32 bar of pressure in section Driver (pressure rupture of diaphragm) and 25 °C of temperature in both section. The membrane was the placed located between the sections Driver (high pressure) and Driven (low pressure), this region is located in the middle of the tube. Was used membranes of aluminum and copper to rupture. The figure 12 shows the membrane of aluminum before the tests.

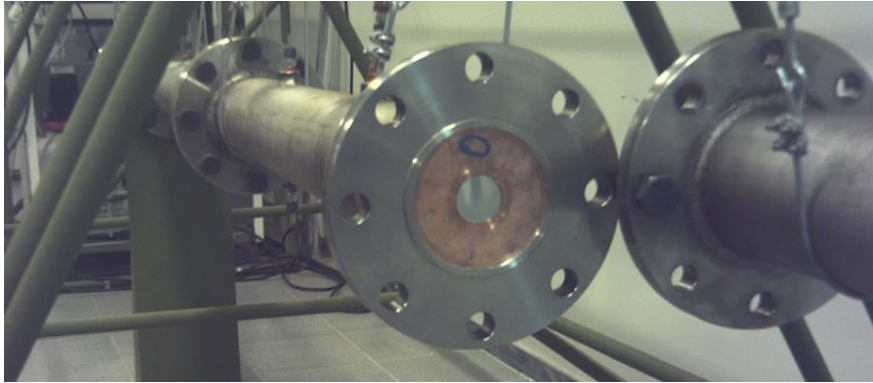


Figure 12 – Membrane of aluminum before the tests in shock tube.

The parameter for the measurement of the ignition delay was given as the start of the shock wave (P1) and the appearance of the light (T1). These beginnings are considered as the point of inflection in the pressure and light curves, it was shown in fig. 9. The curves of both parameters in all tests was acquired in LABVIEW and plotted in the MATLAB. After the inflection points were determined graphically. The ignition delay is the interval between the beginning of the pressure wave in (P1) and the appearance of luminosity (T1) given by Eq.13.

$$\Delta_t = T_1 - P_1 \quad (13)$$

Where:

Δt - ignition delay [ms];

T_1 - Moment when luminosity appear [ms];

P_1 - Moment when the shock wave passage to pressure sensor P1[s].

3 - RESULTS AND DISCUSSION

The table 1 shows the estimate of pressure, temperature, Mach number and speed of propagation shock wave incident and reflective calculated with equation 1 to 12.

Table 1 - Pressure, temperature, Mach number and speed of propagation shock wave incident and reflective.

Driven section		Driver section		Incident shock				Reflective shock			
P4 (bar)	T4 (K)	P1 (bar)	T1 (K)	P2 (bar)	T2 (K)	Mach 2	V2 (m/s)	P5 (bar)	T5 (K)	Mach 5	V5 (m/s)
33.00	300.00	1.00	300.00	9.48	874.90	2.00	689.90	15.06	928.70	1.74	692.70
33.00	300.00	1.00	383.00	9.07	1229.20	1.91	742.20	12.92	1359.40	1.70	661.90
33.00	300.00	1.00	393.00	9.03	1244.70	1.90	748.00	12.71	1374.60	1.69	658.70
33.00	300.00	1.00	403.00	8.99	1260.70	1.89	753.70	12.51	1389.70	1.68	655.70
33.00	300.00	1.00	408.00	8.97	1276.40	1.89	756.50	12.42	1397.20	1.69	654.20
33.00	300.00	1.00	413.00	8.95	1292.70	1.88	759.20	12.32	1404.70	1.68	652.80

Table 2 correlates the tests performed on the shock tube for the measurement of ignition delay time with cetane number of fuel.

Table 2 – measurement of ignition delay time with cetane number of fuel.

Results of test in Shock tube		
Fuel	Ignition delay time (μs)	Cetane number
Diesel S25	200	43
Diesel S25	200	43
Diesel S25	225	43
Diesel S25	200	43
Diesel S25	225	43
Ethanol additive	500	-
Ethanol additive	525	-
Ethanol additive	575	-
Biodiesel B100	975	38
Biodiesel B100	900	38
Biodiesel B100	1225	38
Biodiesel B100	1025	38
Biodiesel B100	1125	38
Diesel Reference	150	52
Diesel Reference	175	52
Diesel Reference	150	52
Not application cetane number to etanol fuel		

The figure 13 presented the ignition delay time of Diesel S25, Ethanol Additive, Biodiesel B100 and Diesel Reference in function of shock temperature.

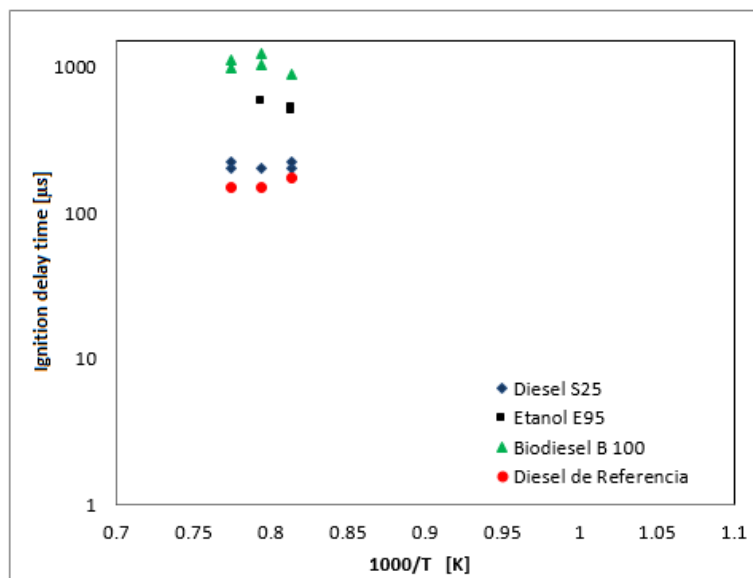


Figure 13 - Ignition delay time of Diesel S25, Ethanol Additive, Biodiesel B100 and Diesel Reference in function of shock temperature.

The delay times measured for Diesel reference ranged from 150 to 175 μs , for Diesel S25 the ranged from 200 to 225 μs , for the Ethanol Additive the ranged from 500 to 575 μs and Biodiesel B100 the ranged from 900 to 1225 μs . The cetane number of Diesel reference is 52.4, the Diesel S25 is 43.00. The Biodiesel B100 is approximate 38 and for Ethanol Additive the cetane number is not application. The ignition delay time is inversely proportional to cetane number, fuel that presented high cetane number have a short ignition delay time and the best quality is the combustion process. The table 2 and figure 13 shows the Diesel reference with minor ignition delay time, this is to be expected because this fuel presented great cetane number. Due the Biodiesel B100 presented minor cetane number, this have a great ignition delay time.

4 – CONCLUSIONS

Measured the ignition delay time of Diesel S25 and Diesel reference, the values were respectively (200-225 μs). The measured values are consistent since reference Diesel has the highest cetane number of the diesel S25. The cetane number is inversely proportional to the duration of the ignition delay time, i.e. the greater the number of cetane lower ignition delay time.

Measured ignition delay time of ethanol with 5 % additive, the values found are in the range (500-575 μs).

Measured ignition delay time of Biodiesel B100, the values found are in the range (900-1225 μs).

Should not use the fuel additive ethanol and B100 biodiesel as substitutes for diesel compression ignition engines without any major changes in engines. The ignition delays times of these fuels are at least three to four times larger than the time delay of the diesel reference. This could cause serious malfunctions of engines, such as clogging of nozzles and hard starting engine. Being necessary to make changes in the construction of them, for example, increased compression ratio.

5 – ACKNOWLEDGEMENTS

PETROBRAS

VALE

FAPEMIG

UNI-BH - CENTRO UNIVERSITARIO DE BELO HORIZONTE

CPGMEC – COLEGIADO DE PÓS-GRADUAÇÃO EM ENGENHARIA MECÂNICA

6 – REFERENCES

- Antonio, M. C. N., 2001- Effect of Piston Gas Pipe / Tunnel Crash When operated in Condition Balance Interface.
- Cancino, L. R. Autoignition of gasoline surrogate mixtures at intermediate temperatures and high pressures: Experimental and numerical approaches. Proceeding of the Combustion institute, 2009.
- McMillan, R.J., 2004- Shock tube investigation of pressure and ion sensors used in pulse detonation engine research.
- Campbell, M.F.; Davidson, D.F.; Hanson, R.K. and Westbrook C.K. Ignition delay times of methyl oleate and methyl linoleate behind reflected shock waves, Stanford, California, USA, 2012.
- Cancino, L.R.; Fikri M.; Oliveira, A.A.M.; Schulz, C. Auto ignition of gasoline surrogate mixtures at intermediate temperatures and high pressures: Experimental and numerical approaches, Duisburg, Germany, 2009.
- Davidson, D. F.; Oehlschlaeger, M. A.; Herbon, J. T. and Hanson, R. K. Shock Tube measurements of Iso-Octane ignition times and oh concentration time histories. High Temperature Gasdynamics Laboratory Mechanical Engineering Department Stanford University, Stanford, California, USA, 2004.

7 - RESPONSIBILITY NOTICE

The authors are the only responsible for the printed material included in this paper.